Proceedings of the 4th International Conference on Functional Materials and Civil Engineering
DOI: 10.54254/2755-2721/2026.38768

A Study on the Minimum Folding Steps and Degrees of Freedom Required for Hamiltonian Cycle Paths

Yuntong Chen[1,*,†], Rongning Fan[2,†], Haole Shen[3,†]

[1]*School of Mechanical Engineering and Automation, Fuzhou University, Fuzhou, China*
[2]*School of Materials Science and Engineering, Shanxi Normal University, Linfen, China*
[3]*Ningbo Foreign Language School, Ningbo, China*
**Corresponding Author. Email: 022501205@fzu.edu.cn*
†These authors contributed equally to this work and should be considered as co-first authors

Abstract. Deployable grid structures are widely used in aerospace engineering due to their capability of compact storage and large-scale deployment. However, the design of efficient folding paths for thick-panel grid structures remains challenging because of the complex relationship between topology and mechanical performance. Hamiltonian cycles provide an effective approach for generating continuous and non-intersecting folding trajectories, but systematic evaluation and optimization of different grid configurations remain limited. This study proposes a topology optimization framework for Hamiltonian-cycle-based thick-panel folding structures. Three rectangular grids, including 4×4, 4×5, and 4×6 configurations, are investigated. A complete enumeration algorithm is developed to generate Hamiltonian cycles, followed by rotational and mirror symmetry elimination to obtain independent topologies. Thickness interference screening, degree- of - freedom (DOF) calculation, and minimum folding-step analysis are further introduced to evaluate folding feasibility and performance. Based on these criteria, optimal Hamiltonian cycle configurations are identified for different grid sizes. The proposed framework integrates graph-based topology generation with kinematic analysis, providing a systematic approach for the design and optimization of compact deployable folding structures.

Keywords: Hamiltonian cycles, thick-panel folding, deployable structure, degree-of-freedom, minimum folding steps

1. Introduction

Deployable grid structures have become an indispensable core component in modern aerospace engineering that could widely adopted in solar wing arrays, space radar panels and on-orbit optical platforms. These planar grid assemblies require compact stowage for rocket launch and full planar unfolding in orbit, which imposes strict constraints on folding path planning, mechanical kinematics and structural stability. Hamiltonian cycle theory originally proposed in graph theory to describe closed paths covering all vertex nodes exactly once. It has recently been introduced into thick-panel grid folding design to generate continuous and non-intersecting folding trajectories.

© 2026 The Authors. This is an open access article distributed under the terms of the Creative Commons Attribution License 4.0 (https://creativecommons.org/licenses/by/4.0/).

DOI: 10.54254/2755-2721/2026.38768

Yang et al. [1] proposed a thick-panel folding and deployment strategy based on Hamiltonian cycles, in which identical rigid panels connected by spring-loaded hinges were arranged according to Hamiltonian trajectories to achieve compact storage and collision-free deployment. This approach was primarily developed for large aerospace deployable array structures, such as solar arrays and reflectarray antennas. Yang [2] further established a systematic framework for origami- and kirigami-adapted thick-panel folding, including folding topology construction, hinge arrangement, and deployment sequence design. These studies demonstrated the potential of Hamiltonian cycles as a topology-based approach for generating continuous folding paths in thick-panel structures.

Beyond Hamiltonian-based folding systems, previous studies on deployable and rigid-folding structures have mainly focused on two complementary aspects: topology generation and mechanical performance evaluation. From the perspective of topology design, Hamiltonian paths and cycles in grid structures have been extensively investigated as fundamental problems in graph theory. Itai et al. [3] studied Hamiltonian paths in grid graphs and established fundamental conditions for their existence, providing a theoretical basis for searching feasible folding structures. Wynn [4] investigated the enumeration of nonisomorphic Hamiltonian cycles on square grid graphs by considering symmetry operations, providing an effective approach for eliminating equivalent configurations during topology classification. These graph-based approaches provide effective tools for generating possible folding layouts and eliminating redundant solutions caused by geometric symmetry.

From the perspective of mechanical analysis, rigid origami and thick-panel folding structures have been investigated through geometric and kinematic modeling approaches. Tachi [5] proposed geometric methods for designing rigid origami structures and analyzing their folding constraints. Schenk and Guest [6] investigated the geometric and mechanical characteristics of origami-inspired structures, demonstrating the importance of mobility analysis and deformation constraints in deployable systems. Demaine and O'Rourke [7] further summarized computational methods for geometric folding problems, providing theoretical foundations for algorithm-based folding analysis. In addition, studies on deployable mechanisms and origami-inspired engineering structures have applied kinematic models to evaluate DOF, motion constraints, and deployment behavior [8-11]. Therefore, existing research on Hamiltonian-cycle-based folding structures can generally be categorized into two interconnected approaches: graph-based topology enumeration for generating feasible folding paths and kinematic mechanism modeling for evaluating their mechanical performance.

Synthesizing the above review of research objects and methodological progress, most papers discuss a single grid specification without horizontal performance comparison of Hamiltonian cycle folding indicators, there remains a gap in current research. Existing research lacks a unified comparative study covering 4×4, 4×5 and 4×6 thick grids and simultaneously complete Hamiltonian cycle enumeration, symmetric duplicate removal, thickness interference filtering, DOF calculation and folding step statistics, and optimal path screening. Most papers only discuss a single grid specification without horizontal performance comparison of Hamiltonian cycle folding indicators.

Aiming at the above unresolved research deficiencies, this paper takes 4×4, 4×5 and 4×6 rectangular grids as the research carrier to complete a full set of topological screening and performance evaluation work. Firstly，a complete enumeration algorithm is constructed to generate all Hamiltonian cycles of the three types of grids, and mirror and rotational symmetric equivalent cycles are eliminated to retain independent unique topologies. Secondly, the mobility formula is used to calculate the DOF of each independent cycle mechanism, and the panel folding motion sequence is disassembled to count the minimum folding steps required for full stacking. Finally, all

DOI: 10.54254/2755-2721/2026.38768

unique cycles are ranked by two performance indicators, and the optimal Hamiltonian cycle layout with the smallest DOF and the least folding steps is screened out for each grid size, forming a standardized topology optimization process for grid folding structures.

2. Method analysis

2.1. Path calculation

A series of initial conditions are prescribed in this paper for dynamic simulation of the foldable array: set a starting point, move one step at a time into each visited area from the starting point, only moving one square per step, without retracing the same direction, covering every square exactly once, and finally returning to the starting point, and Python codes are developed based on these conditions. The python code is adopted to implement Hamiltonian cycle enumeration, symmetry elimination and thickness-interference filtering. The core implementation codes are provided in Appendix A. It is concluded that there are two inequivalent paths in the 4×4 Hamiltonian cycle. They can be observed in Figure 1.

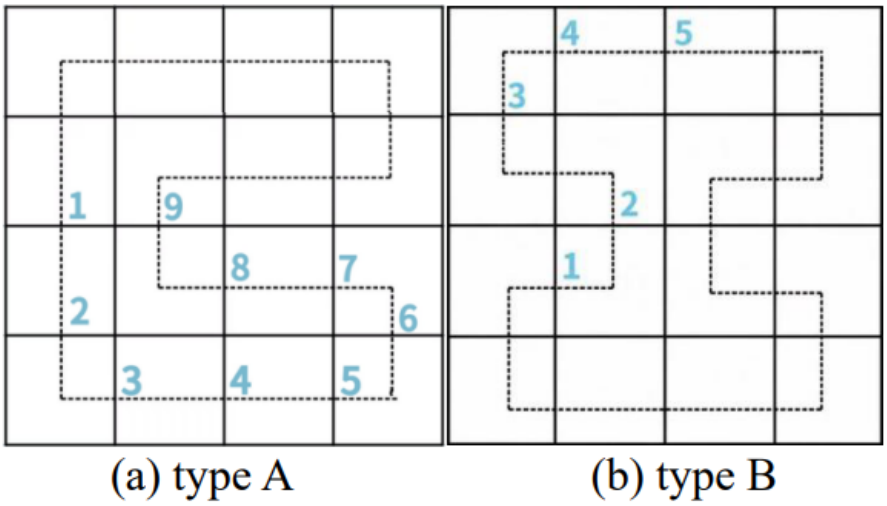


Figure 1. Two types of 4×4 hamiltonian cycle

If two adjacent panels connected in the Hamiltonian cycle are set as the base, numerous starting-point positions are available in Figure 1(a) type A, which gives rise to many distinct paths. However, after eliminating mirrored and symmetric configurations, only nine inequivalent bases actually exist for Figure 1(a) type A, as shown in the figure. By the same reasoning, after removing symmetric and mirrored cases for Figure 1(b) type B, only five inequivalent bases remain.

2.2. Physical prototyping and experimental validation

This paper first takes the nine different bases in Figure 1(a) type A as the research objects. Vector-reflection method is adopted to calculate whether each base can be folded into a double-stacking configuration.

DOI: 10.54254/2755-2721/2026.38768

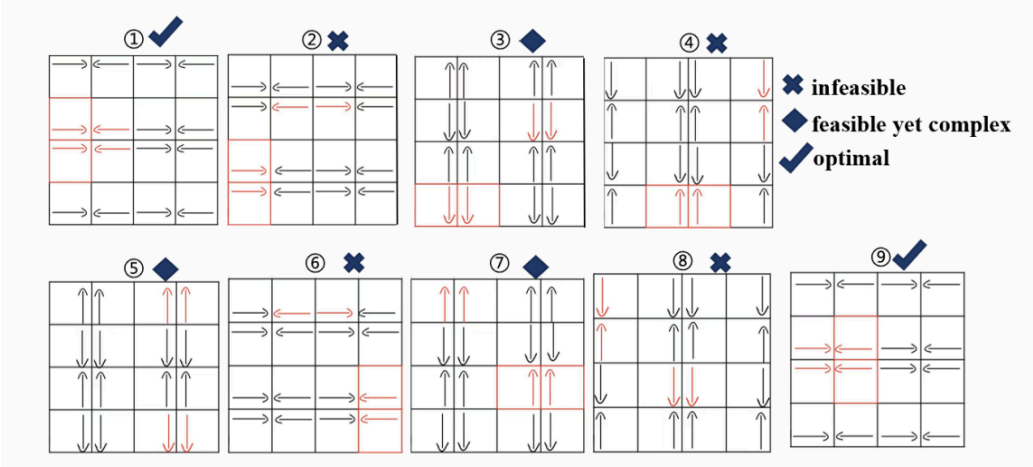


Figure 2. Nine distinct bases of 4×4 type A

As can be seen from the Figure 2., this paper classifies the paths into three categories: infeasible, feasible yet complex, and optimal. Specifically, infeasible bases cannot be folded into a double-stacking structure. Feasible yet complex bases can achieve double-stacking structure but require numerous folding steps and possess high DOF, leading to difficult control. Optimal bases can be folded into double-stacking configurations with fewer steps and low DOF for easy control.

For Figure 2, there are four infeasible configurations, three feasible yet complex configurations and two optimal configurations in total.

Since infeasible configurations cannot complete folding, this paper does not focus on their DOF and folding steps. Next are the feasible yet complex configurations. Taking base No.⑦ of Figure 2 as an example, Figure 3(b) and Figure 3(c) show the exploded views of its corresponding physical paper model, the former corresponds to the front side, while the latter is the rear side. During the folding process of feasible yet complex configurations, up to four panels can be merged into two rectangular panels. For instance, the four panels marked with red arrows in base of Figure 3(a) can be combined into two rectangular panels, which reduces the DOF and folding steps to a certain extent. According to calculations, the three feasible yet complex configurations of Figure 1(a) type A all have a DOF of 8.

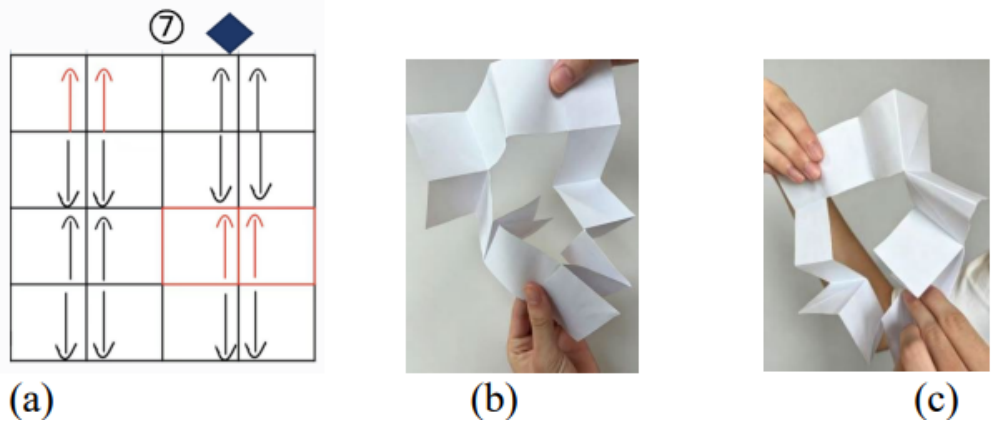


Figure 3. Base No. 7 of Type A and the deployed view of its paper model

Taking the optimal configuration presented in Figure 4 as an example, eight panels can be merged into four rectangular panels in its vector-reflection diagram, which greatly reduces the DOF and

DOI: 10.54254/2755-2721/2026.38768

folding steps. According to calculations, all optimal configurations of Figure 1(a) type A have a DOF of 6 and require five folding steps.

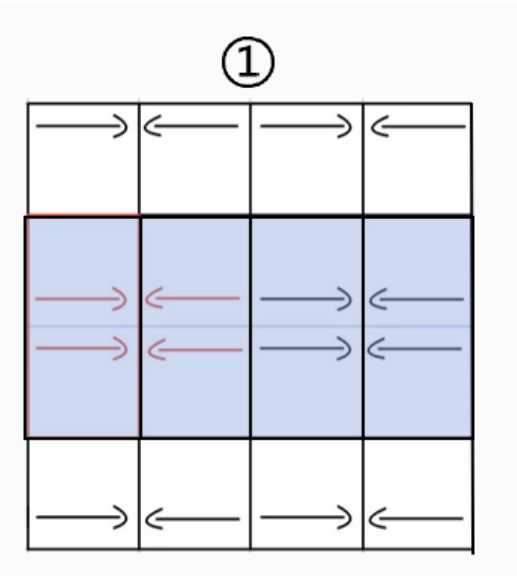


Figure 4. Base No. 1 of type A

The same method is adopted in this paper to analyze type B, which has five distinct paths in total. Figure 1(b) type B contains three feasible yet complex configurations and two optimal configurations.

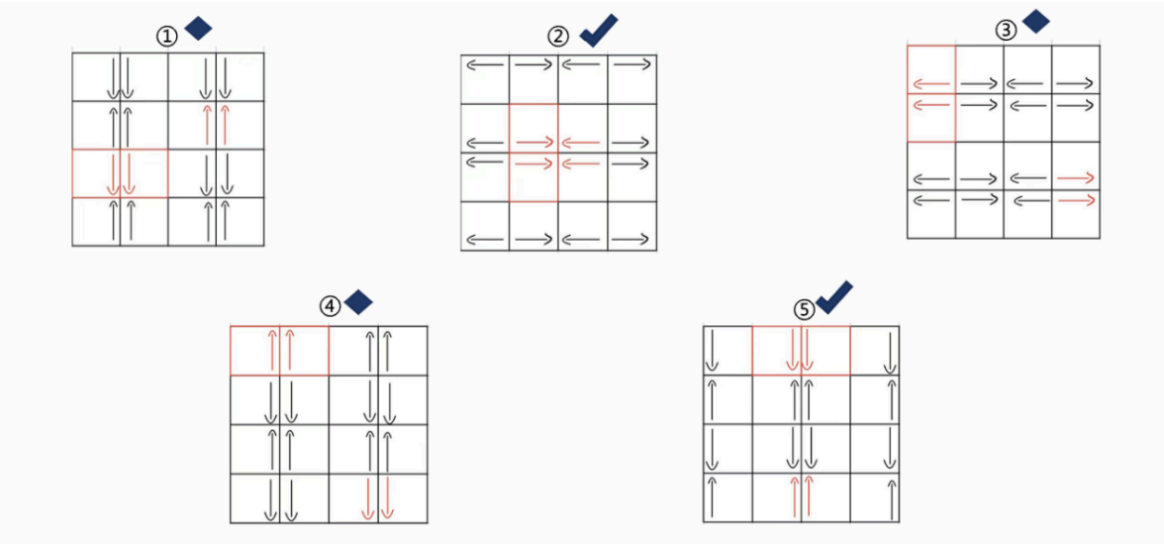


Figure 5. Five distinct bases of type B

Taking base No.④ of Figure 5 as an example, Figure 6(b) and Figure 6(c) show the exploded views of its corresponding physical paper model, the former corresponds to the front side, while the latter is the rear side. During the folding process of feasible yet complex configurations, up to four panels can be merged into two rectangular panels. For instance, the four panels marked with red arrows in base of Figure 6(a) can be combined into two rectangular panels, which reduces the DOF

DOI: 10.54254/2755-2721/2026.38768

and folding steps to a certain extent. According to calculations, the three feasible yet complex configurations of type B all have a DOF of 8.

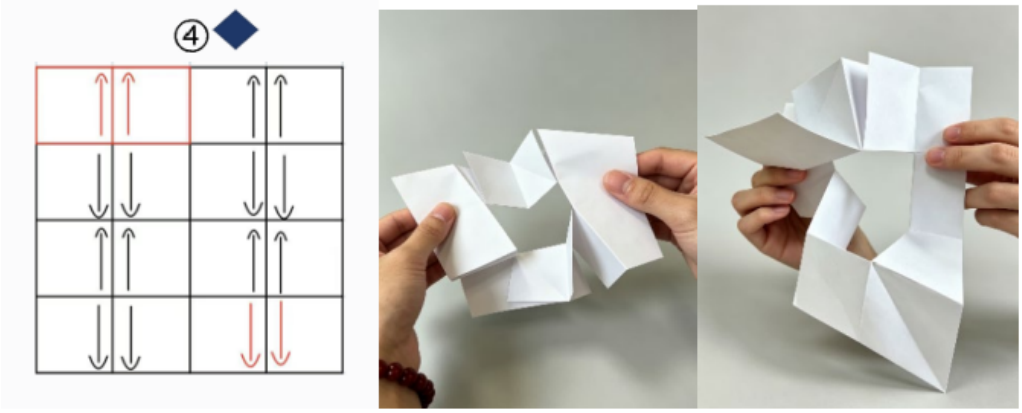


Figure 6. Base No. 1 of type B and the deployed view of its paper model

Taking the optimal configuration presented in Figure 7 as an example, eight panels can be merged into four rectangular panels in its vector-reflection diagram, which greatly reduces the DOF and folding steps. According to calculations, all optimal configurations of type B have a DOF of 6 and require five folding steps.

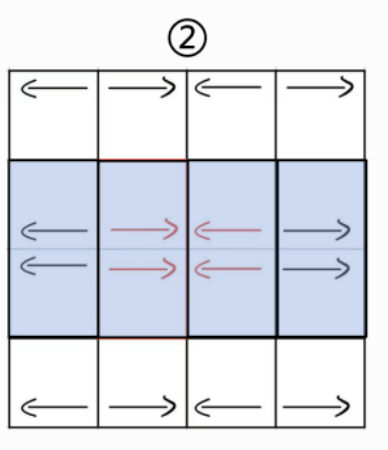


Figure 7. Base No. 2 of type B

2.3. Calculation of DOF

For the optimal configurations in type-A and type-B, let N denote the number of links and J denote the number of joints, where each joint has f_i rotational DOF.

$$N = 12 \tag{2.1}$$

$$J = 12 \tag{2.2}$$

DOI: 10.54254/2755-2721/2026.38768

$$M = \left(6 - J - N - 1\right) + \sum_{i=1}^{J} f_i = 6 \tag{2.3}$$

3. Extension and validation

3.1. Observation

Based on the above research, it can be clearly observed that the best solution among all 4×4 Hamiltonian cycles is composed of both rectangles and squares in Figure 8. It is further conjectured whether this possible to find a Hamiltonian cycle constructed solely of rectangles to dramatically reduce the DOF.

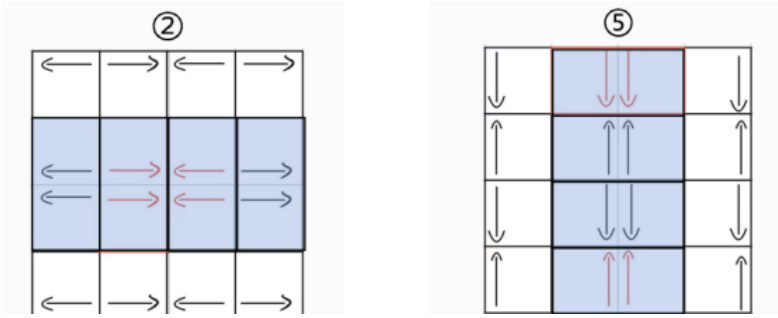


Figure 8. Best solutions for the 4×4 configuration

When converting the Hamiltonian cycle of the 4×4 grid composed entirely of square panels into one consisting solely of rectangular panels, merely a single path is available. The Hamiltonian cycle of the 4×4 grid is illustrated in Figure 9.

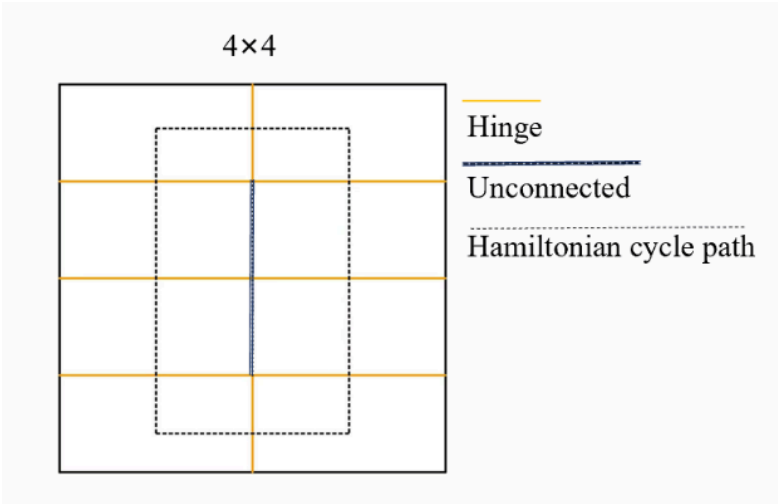


Figure 9. 4×4 grid consisting solely of rectangular panels

To explore additional structural possibilities beyond the 4×4 grid, the grid dimension is expanded, and a full 4×5 Hamiltonian cycle consisting entirely of rectangular panels is established for comparative analysis. Correspondingly, merely one valid path can be obtained in Figure 10.

DOI: 10.54254/2755-2721/2026.38768

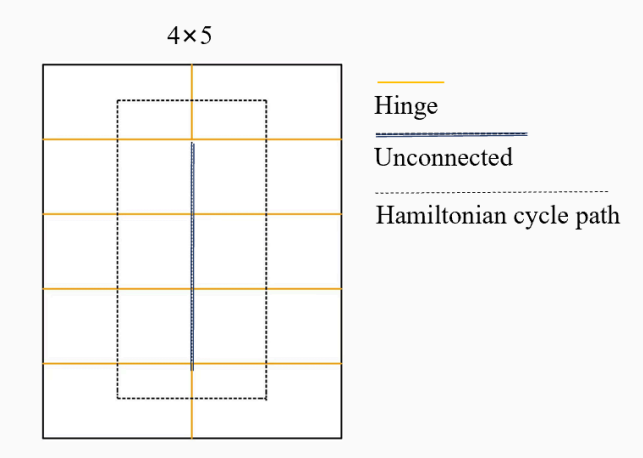


Figure 10. 4×5 grid consisting solely of rectangular panels

As shown in the Figure 9 and Figure 10, neither of them can be folded into a double-stacking structure. Accordingly, it is necessary to revert to the normal method to find the best solution in 4×5.

3.2. 5 types of Hamiltonian cycles of 4×5

A total of five distinct Hamiltonian cycles are available in Figure 11 [12]. The vector reflection method is adopted to verify whether a double-stacking structure can be formed [13]. Meanwhile, this folding scheme is required to minimize both the DOF and folding steps. All pairs of adjacent square panels in each grid are defined as the base units, with two corresponding top units matched to each base unit, so that the overall structural layout can satisfy geometric compatibility constraints while maintaining high assembly efficiency during the origami-based deployment process.

Validation is carried out by flipping the panels upward and downward. For the five distinct Hamiltonian cycles, a total of 73 folding configurations are generated by adopting different base panels. Among these configurations, 44 fail to form a double-stacking structure; 23 are capable of forming such a structure yet remain complicated, characterized by excessive folding steps and high DOF; only six configurations are identified as optimal solutions. All six folding configurations possess 9 DOF and 8 folding steps, which meet the expected design requirements in Table 1.

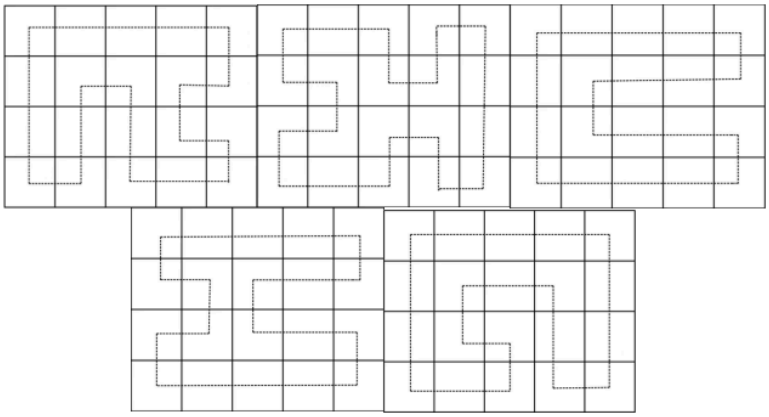


Figure 11. 5 types of Hamiltonian cycles of 4×5 grid

DOI: 10.54254/2755-2721/2026.38768

Table 1. All Configurations with different adjacent panels as the base for the 4×5 grid

	type		
scale	infeasible	feasible yet complex	optimal
4×5	44	23	6

A sample of the six optimal types. Folding is carried out with panels (2,1) and (3,1) defined as the base units, and panels (2,2) and (3,2) as the corresponding top units in Figure 12(a). Figure 12(b) is the vector diagram corresponding to the 4×5 grid where the blue-shaded areas represent the five rectangular panels. Employing as many rectangular panels as possible can minimize the DOF and folding steps during the folding procedure.

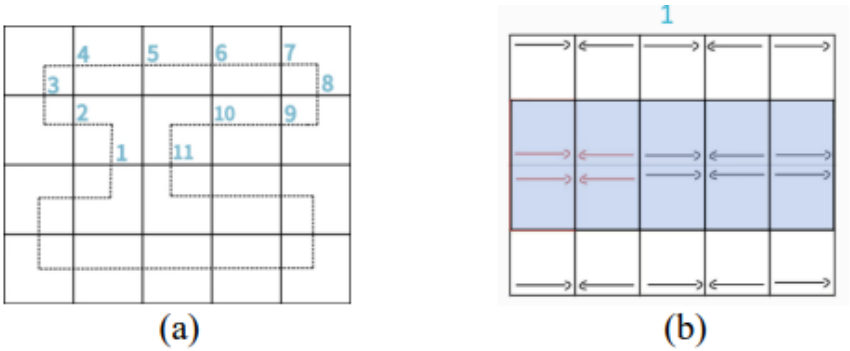


Figure 12. One of 4×5 Hamiltonian cycle path and corresponding vector plot

The optimal solution for 4×5 is still composed of both rectangles and squares. Continue to extend to a 4×6 scale.

3.3. 4×6 Hamiltonian cycles

To satisfy the constraints of Hamiltonian cycles, namely, to form a closed loop that visits every vertex of a graph exactly once and returns to the starting vertex, with each consecutive pair of vertices connected by an edge in the graph. Only two feasible paths are available. Evidently, the path illustrated in Figure 13(a) fails to form a double stacking structure, and the path in Figure 13 (b) is subsequently discussed.

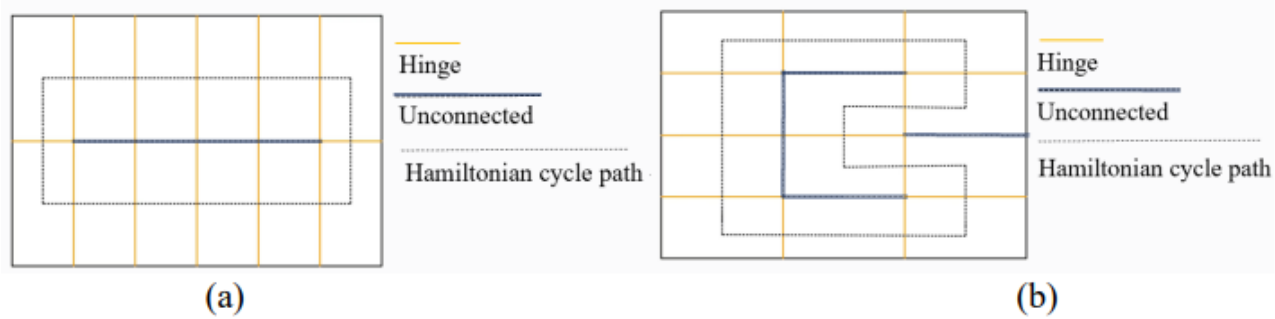


Figure 13. 4×6 grid consisting solely of rectangular panels

Topological Criteria for the Realization of a Double-Stacking Configuration: Divide grid units into two separate non-interleaved layer groups. When two adjacent rectangular units are set as the

DOI: 10.54254/2755-2721/2026.38768

base and top layers respectively, the two units are linked by a continuous hinge path within the intact Hamiltonian cycle. The realization of double-stacking demands the partition of these two units into two independent folding regions. Nevertheless, such a continuous cyclic path cannot be segmented. If the integrity of the Hamiltonian cycle is maintained, the interlinked intermediate panels will give rise to spatial interference and disordered layering, which prevents the formation of a standard double-stacking configuration. One of the folding schemes is demonstrated in Figure 14.

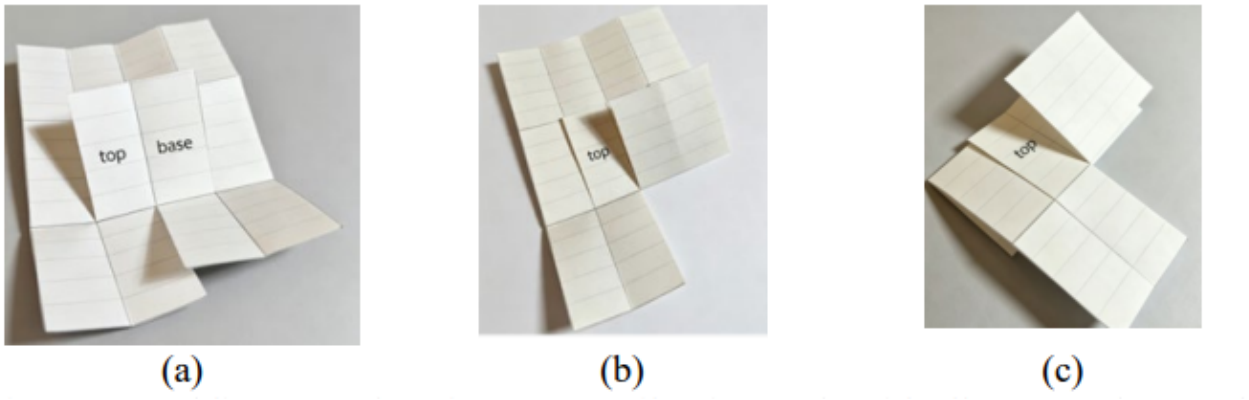


Figure 14. Folding procedure for 4×6 Hamiltonian cycle with all-rectangular panels

As can be seen from Figure 14(a), folding is implemented by taking one panel as the base and its adjacent panel as the top. In Figure 14(b) if the front two panels are folded upward in advance, the remaining four panels can only be folded downward, and this folding sequence yields the configuration shown in Figure 14(c). Under this circumstance, panels exist on both the upper and lower sides of the base panel, which fails to meet the structural requirements. It is possible to obtain cycle-adjacent units are connected in a single continuous chain, which cannot be split into two separate layers. Consequently, the double-stacking structure cannot be achieved for the cycle consisting exclusively of rectangular panels if the completeness of the Hamiltonian cycle is maintained.

Reverting to the normal folding method yields the optimal configurations for the 4×6 grid specification.

Owing to the large number of Hamiltonian cycles generated by the 4×6 grid structure, only symmetric configurations are discussed in this section, among which five distinct types of Hamiltonian cycles are identified [1]. The five distinct types of Hamiltonian cycles are demonstrated in Figure 15. Consistent with the research methodology adopted for the 4×5 grid, configurations that can form a double-stacking structure while minimizing both DOF and folding steps are explored. Folding verification is implemented by taking every pair of adjacent square panels as the base units. A total of 53 folding cases with different base units are obtained. Among all these cases, 14 are unable to form a double-stacking configuration; 33 can realize the target double-stacking structure yet exhibit high complexity with excessive folding steps and large DOF; the remaining six cases correspond to optimal solutions in Table 2. All six folding configurations possess 12 DOF and 11 folding steps, which meet the expected design requirements.

DOI: 10.54254/2755-2721/2026.38768

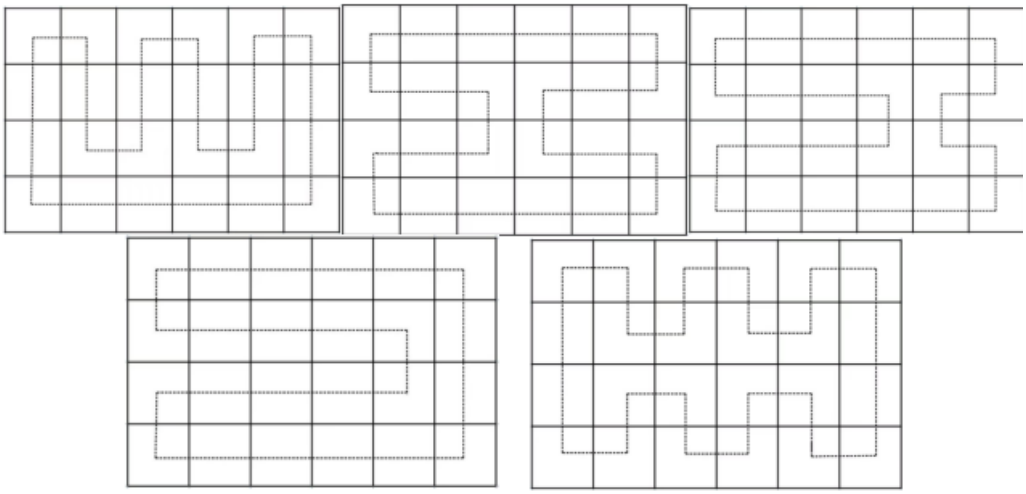


Figure 15. 5 types of Hamiltonian cycles of 4×6 grid

Table 2. All configurations with different adjacent panels as the base for the 4×6 grid

	type		
scale	infeasible	feasible yet complex	optimal
4×6	14	33	6

A sample of the six optimal types. Folding is carried out with panels (2,5) and (3,5) defined as the base units, and panels (2,6) and (3,6) as the corresponding top units in Figure 16(a). Figure 16(a) is one of 4×6 Hamiltonian cycle path and figure 16(b) is corresponding vector plot. The five rectangular wooden panels are represented by the blue-shaded areas in the corresponding vector diagram of the 4×6 grid. Employing as many rectangular panels as possible can minimize the DOF and folding steps during the folding procedure. Figure 17 illustrates the folding process of this sample.

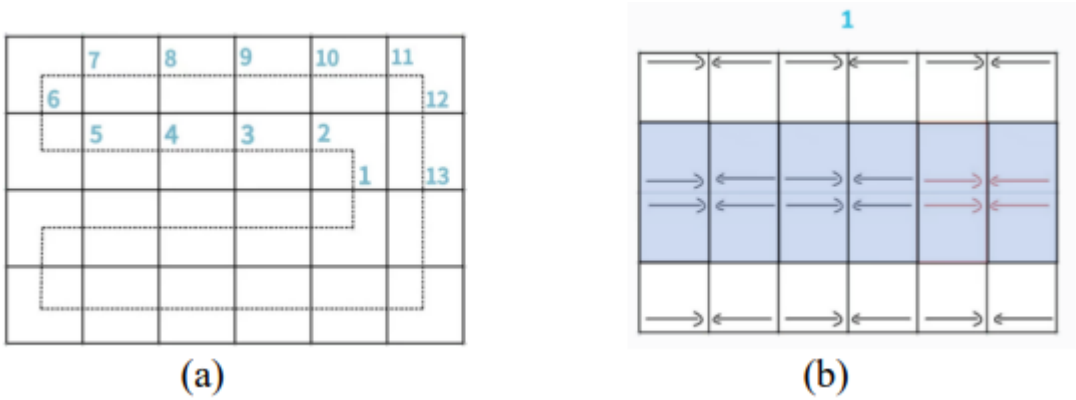


Figure 16. One of 4×6 Hamiltonian cycle path and corresponding vector plot

DOI: 10.54254/2755-2721/2026.38768

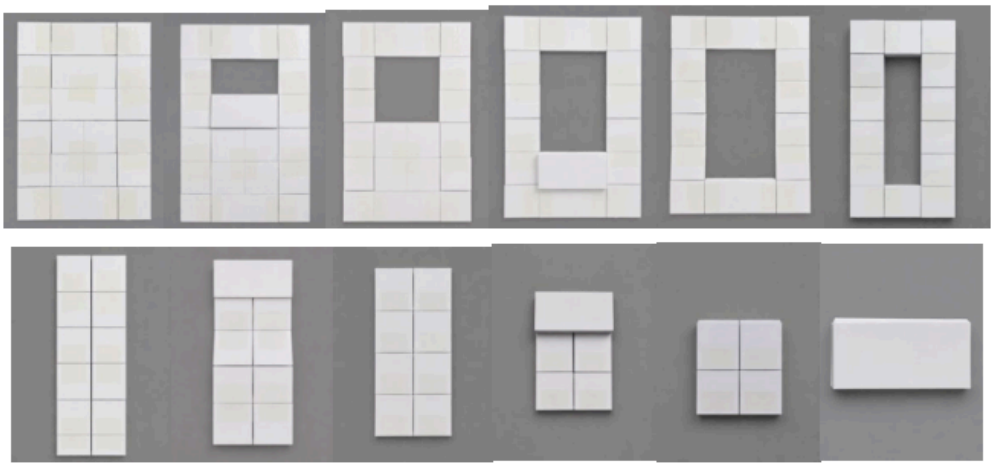


Figure 17. Folding process of a sample of the six optimal types

Under the specification of 4×6, the best solution is still composed of both rectangles and squares.

4. Conclusion

Among the best solutions obtained by minimizing both the DOF and folding steps for Hamiltonian cycles in the 4×4, 4×5 and 4×6 configurations, the panels are arranged as a combination of squares and rectangles to form Hamiltonian cycles, rather than consisting solely of squares or solely of rectangles. As illustrated in Figure 8, the panels adopt mixed square-rectangle arrangement.

For the 4×4 Hamiltonian cycles, there exist 4 infeasible configurations, 6 feasible-yet-complex configurations and 4 optimal configurations. The optimal configurations possess a minimum DOF of 6 with 5 folding steps. For the 4×5 Hamiltonian cycle, the numbers are 44 infeasible, 23 feasible-yet-complex and 6 optimal configurations; the optimal configurations achieve a minimum DOF of 9 and require 8 folding steps. For the symmetric 4×6 Hamiltonian cycle, 14 infeasible, 33 feasible-yet-complex and 6 optimal configurations are obtained. The optimal configurations have a minimum DOF of 12 and 11 folding steps.

References

[1] Yang, J., Zhang, Y., Chatzis, M. N., & You, Z. (2022). Folding and deploying identical thick panels with spring-loaded hinges. *Extreme Mechanics Letters, 52*, 101637.
[2] Yang, J. (2022). *Origami- and kirigami-adapted thick-panel folding*. PhD thesis, University of Oxford.
[3] Itai, A., Papadimitriou, C. H., & Szwarcfiter, J. L. (1982). Hamilton paths in grid graphs. *SIAM Journal on Computing, 11*(4), 676–686.
[4] Wynn, E. (2014). Enumeration of nonisomorphic Hamiltonian cycles on square grid graphs. arXiv:1402.0545.
[5] Tachi, T. (2010). Geometric considerations for the design of rigid origami structures. *Proceedings of the International Association for Shell and Spatial Structures (IASS) Symposium*.
[6] Schenk, M., & Guest, S. D. (2013). Geometry of Miura-folded metamaterials. *Proceedings of the National Academy of Sciences, 110*(9), 3276–3281.
[7] Demaine, E. D., & O'Rourke, J. (2007). *Geometric folding algorithms: Linkages, origami, polyhedra*. Cambridge University Press.
[8] Guest, S. D., & Pellegrino, S. (1994). The folding of triangulated cylinders, part I: Geometry. *Journal of Applied Mechanics, 61*(4), 773–777.
[9] Hoberman, C. (1990). *Reversibly transformable structures*. United States Patent.
[10] Miura, K. (1980). *Method of packaging and deployment of large membranes in space*. Institute of Space and Astronautical Science.

DOI: 10.54254/2755-2721/2026.38768

[11] Kuribayashi, K., Tsuchiya, K., You, Z., Tomus, D., Umemoto, M., Ito, T., & Sasaki, M. (2006). Self-deployable origami stent grafts as a biomedical application of Ni-rich TiNi shape memory alloy foil. *Materials Science and Engineering: A, 419*, 131–137.

[12] Qian, Z., Zhong, Q., Zhang, Q., & Cai, J. (2026). Configuration design and dynamics analysis of large-scale planar deployable antenna based on Hamiltonian circuits. *Space Solar Power and Wireless Transmission*. https://doi.org/10.1016/j.sspwt.2026.03.001

[13] Gogu, G. (2005). Chebychev–Grübler–Kutzbach's criterion for mobility calculation of multi-loop mechanisms revisited via theory of linear transformations. *European Journal of Mechanics - A/Solids, 4*(3), 27–441. https://doi.org/10.1016/j.euromechsol.2004.12.003